Developmental Biology 324 (2008) 10–17

Contents lists available at ScienceDirect

Developmental Biology

journal homepage: www.elsevier.com/developmentalbiology

WNT5A selectively inhibits mouse ventral prostate development

Sarah Hicks Allgeier [a], Tien-Min Lin [b], Chad M. Vezina [b], Robert W. Moore [a,b], Wayne A. Fritz [b], Shing-Yan Chiu [c], ChuanLi Zhang [c], Richard E. Peterson [a,b,*]

[a] Molecular and Environmental Toxicology Center, University of Wisconsin, Madison, WI 53705, USA
[b] School of Pharmacy, University of Wisconsin, Madison, WI 53705, USA
[c] Department of Physiology, University of Wisconsin, Madison, WI 53705, USA

ARTICLE INFO

Article history:
Received for publication 30 October 2007
Revised 8 August 2008
Accepted 18 August 2008
Available online 29 August 2008

Keywords:
WNT5A
TCDD
Urogenital sinus
Ventral prostate development
Prostatic bud formation
Mouse

ABSTRACT

The establishment of prostatic budding patterns occurs early in prostate development but mechanisms responsible for this event are poorly understood. We investigated the role of WNT5A in patterning prostatic buds as they emerge from the fetal mouse urogenital sinus (UGS). *Wnt5a* mRNA was expressed in UGS mesenchyme during budding and was focally up-regulated as buds emerged from the anterior, dorsolateral, and ventral UGS regions. We observed abnormal UGS morphology and prostatic bud patterns in *Wnt5a* null male fetuses, demonstrated that prostatic bud number was decreased by recombinant mouse WNT5A protein during wild type UGS morphogenesis *in vitro*, and showed that ventral prostate development was selectively impaired when these WNT5A-treated UGSs were grafted under under kidney capsules of immunodeficient mice and grown for 28 d. Moreover, a WNT5A inhibitory antibody, added to UGS organ culture media, rescued prostatic budding from inhibition by a ventral prostatic bud inhibitor, 2,3,8,7-tetrachlorodibenzo-*p*-dioxin, and restored ventral prostate morphogenesis when these tissues were grafted under immunodeficient mouse kidney capsules and grown for 28 d. These results suggest that WNT5A participates in prostatic bud patterning by restricting mouse ventral prostate development.

Introduction

The mature mouse prostate is comprised of four bilaterally symmetric lobes: anterior, dorsal, lateral and ventral. Each prostate lobe features unique ductal morphology and gene expression profiles, yet they all arise from a common primordium, the urogenital sinus (UGS). Specification of prostate lobar identity begins during embryogenesis and is mediated by androgen-dependent interactions between UGS mesenchyme (UGM), and UGS epithelium, UGE (Cunha et al., 1987). These interactions promote outgrowth of ductal precursors, or buds, that derive from UGE in a distinct spatial pattern and temporal sequence (Lin et al., 2001). Buds on the anterior UGE surface emerge first, as early as embryonic day (E) 16.5, and give rise to anterior prostate ducts. Dorsal prostate buds also emerge on E16.5 and lateral and ventral buds are the last to appear on approximately E17.5.

Budding is a recurrent theme in limb, lung, tooth, and feather development (Hogan, 1999). While morphogenetic signals often overlap in these tissues, prostate induction is distinguished by its androgen-dependence. Androgen receptors (ARs) in UGM are necessary for bud initiation and UGM is also largely responsible for specifying bud patterns (Cunha and Chung, 1981; Cunha and Lung, 1978; Goldstein and Wilson, 1975).

The most fundamental aspect of the prostatic budding mechanism, how activation of ARs by fetal testosterone participates in bud initiation and patterning, remains unknown. This issue is being addressed by complementary approaches. The first, a chemical genetics approach, uses chemical inhibitors of prostatic budding that act in a region-selective fashion. This approach has revealed some molecular signals involved in prostatic bud patterning. Estrogen receptors were implicated in dorsolateral prostatic budding when it was discovered that estrogen receptor agonists, diethylstilbesterol and bisphenol A, inhibited dorsolateral bud formation (Timms et al., 2005). The nuclear orphan receptor, aryl hydrocarbon receptor (AHR), was implicated in ventral prostatic budding after it was discovered that ventral buds were selectively impaired by the AHR agonist, 2,3,7,8-tetrachlorodibenzo-*p*-dioxin, TCDD (Lin et al., 2003).

The use of transgenic mice and *in vitro* models of prostate growth have also elucidated signaling factors participating in prostate induction and patterning. ARs are required for prostate budding in all UGS zones (Lasnitzki and Mizuno, 1980); fibroblast growth factor 10 (*Fgf10*) is required for the formation of most buds (Donjacour et al., 2003); *Noggin* is required for ventral and anterior prostatic buds (Cook et al., 2007); Sry box 9 (*Sox9*) is required for ventral buds and likely also for other buds (Thomsen et al., 2008), homeobox (*Hox*) *a13* and *d13* are involved in budding in all zones (Podlasek et al., 1999b) but

* Corresponding author. UW-Madison, School of Pharmacy, 777 Highland Ave., Madison, WI 53705, USA.
E-mail address: repeterson@pharmacy.wisc.edu (R.E. Peterson).

0012-1606/$ – see front matter © 2008 Elsevier Inc. All rights reserved.
doi:10.1016/j.ydbio.2008.08.018

are especially important for anterior prostatic budding (Warot et al., 1997). Also involved in prostatic budding are sonic hedgehog (SHH) and retinoic acid, which are prostatic bud agonists and bone morphogenetic proteins (BMPs) 4 and 7, which are prostatic bud antagonists (Doles et al., 2006; Grishina et al., 2005; Lamm et al., 2002; Podlasek et al., 1999a; Vezina et al., 2008). It is unclear at this time how AR, FGF, SHH, BMP, and HOX signals are orchestrated to initiate buds and establish prostatic bud patterns. None of these signals can account completely for the generation of prostatic bud patterns, suggesting that additional factors or coordinated interactions of multiple signals are involved.

Genes of the wingless-related MMTV integration site (*Wnt)* superfamily have been associated with bud initiation and patterning in multiple tissues (Gat et al., 1998; Liu et al., 2008; Liu et al., 2007; Lu et al., 2004; Noramly et al., 1999; Teuliere et al., 2005; Widelitz et al., 2000). WNTs are embedded in a molecular signaling pathway that interfaces with FGF, SHH, BMP, and HOX signaling. Further, *Wnts* are also expressed in the UGS during prostatic budding (Joesting et al., 2008; Zhang et al., 2006), but their role in prostatic bud initiation had not been investigated.

Secreted *Wnts* bind to receptors on target tissues and initiate signaling through two principle mechanisms: a canonical signaling pathway involving stabilization of β-catenin, and a less understood non-canonical, β-catenin-independent signaling pathway. *Wnt5a*, the most abundantly expressed *Wnt* gene in the UGS (Zhang et al., 2006), signals through the non-canonical pathway and its deletion has been shown to impede budding in other developing mouse tissues (Yamaguchi et al., 1999).

In the present study, we sought to determine whether *Wnt5a* is involved in prostatic bud initiation and patterning in the male fetal mouse UGS. We characterized *Wnt5a* mRNA expression in the UGS, assessed development of the UGS and related structures in the *Wnt5a* null fetus, and evaluated the effects of exogenous WNT5A protein and WNT5A inhibitory antibody on prostatic bud formation and patterning in UGS organ culture. The significance of our findings is that they reveal for the first time that WNT5A signaling participates in prostatic bud patterning by restricting ventral prostatic bud formation during prostate morphogenesis.

Materials and methods

Animals

Wnt5a null mice, backcrossed onto a C57BL/6 background (Yamaguchi et al., 1999), were obtained from Terry Yamaguchi (NCI, Frederick, MD). Offspring were genotyped as previously described (Benedict et al., 2000) using the following primers to identify heterozygous breeders: mouse WNT5A primer 5′-TTCCAAGTTCTTCC-TAATGGC-3′ and *E. coli* neomycin resistance cassette primer 5′-TTGGGTGGAGAGGCTATTCG-3′. C57BL/6J wild-type mice were from the Jackson Laboratory (Bar Harbor, ME). Animals were housed with a 12 h light–dark cycle (lighted 0600 to 1800 h) at room temperature (22±1 °C) in clear plastic microisolator cages with corn-cob bedding. Feed (5015 Mouse Diet, PMI Nutrition International, Brentwood, MO) and water were available *ad libitum*.

Timed-pregnant females were generated by housing males and females together overnight. The day after overnight mating was designated E0.5. Pregnant dams were treated as described below, then euthanized by CO_2 overdose prior to removal of fetuses. UGS samples in each experimental block were taken from separate litters to minimize litter-dependent observations. Some pregnant dams were exposed to the ventral prostatic budding inhibitor TCDD (5 μg/kg, po). Dosing occurred on either E13.5 or E15.5, either of which has been shown previously to inhibit ventral bud formation (Vezina et al., in press). All procedures were approved by the University of Wisconsin Institutional Animal Care and Use Committee.

Vibratome sectioning and sectional in situ hybridization

UGSs were fixed overnight in 4% paraformaldehyde, dehydrated in methanol, rehydrated in phosphate-buffered saline containing 0.1% Tween-20 (PBT), embedded in 4% SeaPlaque agarose in PBT (Biowhittaker Molecular Applications, Rockland, ME), and cut into 80 μm sections using a double-edged razor mounted on a vibratome emersed in PBT. *In situ* hybridization was performed on UGS sections as described by Vezina et al. (in press). The *Wnt5a* riboprobe was a gift from Dr. Terry Yamaguchi (NCI, Frederick, MD).

Scanning electron microscopy and bud counting

UGS samples were prepared for scanning electron microscopy (SEM) as previously described (Lin et al., 2003). For experiments involving bud counting, at least four views of each UGS were obtained such that all surfaces of the UGS could be viewed. Two reviewers independently counted the total number of buds for each UGS and these counts were averaged to give the best estimate of actual bud number for each. At least five UGSs were examined in this manner for each treatment group.

Testicular testosterone content

Testicular testosterone content was measured with the Correlate-EIA Testosterone Enzyme Immunoassay Kit (Assay Designs, Inc., Ann Arbor, MI). Steroids were extracted from E18.5 fetal testes with ethyl acetate, extracts were dried and reconstituted in manufacturer supplied buffer, and testicular content was measured according to the manufacturer's instructions. Results are presented as the mean± SEM for 7 litter-independent males of each genotype.

UGS organ culture

E14.5 UGSs were collected and cultured as described previously (Vezina et al., 2008). Cultured UGSs were exposed to 10 nM 5α-dihydrotestosterone (DHT, Sigma) and either dimethyl sulfoxide (DMSO, 0.1% v/v) or 1 nM TCDD dissolved in 0.1% DMSO. Some cultures were also exposed to graded concentrations of recombinant mouse WNT5A protein (rmWNT5A [80% purity], 0.5, 1, or 2 μg/ml; R and D Systems, Minneapolis, MN), goat anti-mouse WNT5A inhibitory antibody (anti-WNT5A-IgG, 4 or 8 μg/ml; R and D Systems), or rmWNT5A (2 μg/ml)+ anti-WNT5A-IgG (8 μg/ml). Anti-WNT5A-IgG was certified to exhibit less than 2% cross-reactivity with WNT4 and WNT10b by the manufacturer. Media and treatments were replaced every 48 h.

Renal grafting

E14.5 UGSs cultured for 3 d as described above, or E18.5 UGSs removed from WT male and *Wnt5a* null male fetuses were grafted under the renal capsules of adult male *nu/nu* immunodeficient mice (Harlan, Indianapolis, IN). Mice received oral antibiotics (Sulfatrim Suspension, Alpharma, Fort Lee, NJ) for one week following surgery. Grafts were removed after 28 d and either fixed with formalin, dehydrated in ethanol, and embedded in paraffin for histology or frozen in liquid nitrogen and stored at −80°C for RT-PCR.

Calcium imaging

To assess rmWNT5A and anti-WNT5A-IgG activity, mouse embryonic fibroblasts (MEFs) were obtained from American Tissue Type Culture Collection (Manassas, VA). MEFs were seeded on 35 mm tissue culture dishes 24 h prior to measurement of intracellular free calcium. MEFs were cultured in Dulbecco's Minimal Essential Medium supplemented with 10% heat-inactivated fetal bovine serum, and

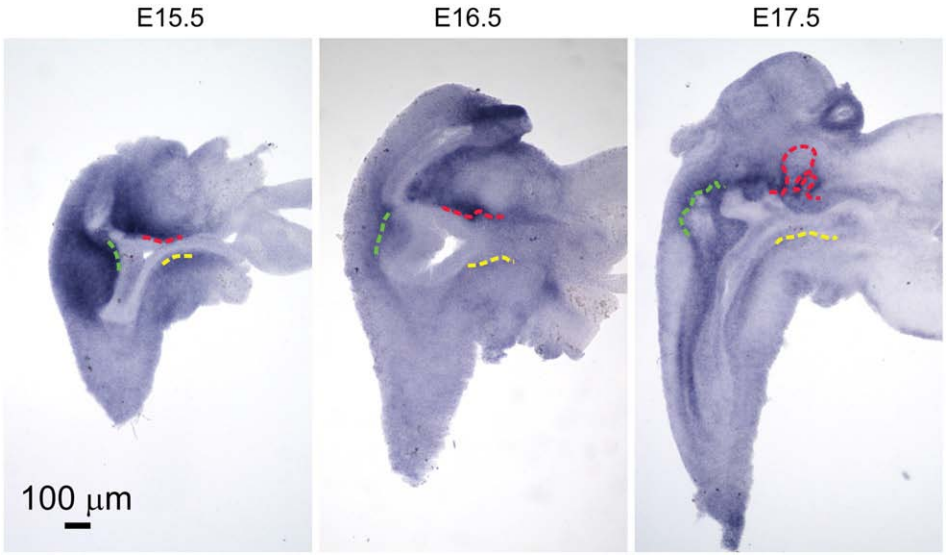

Fig. 1. *Wnt5a* transcripts are expressed in male mouse UGS mesenchyme (UGM) during prostatic bud formation and are increased focally where buds emerge from each UGS zone. *Wnt5a* mRNA distribution was determined by *in-situ* hybridization (ISH) of mid-sagittal male UGS tissue sections at E15.5, 16.5, and 17.5. Results are representative of three UGSs from each day. Colored dashed lines demarcate the UGE-UGM interface in the anterior (red), dorsolateral (green), and ventral (yellow) prostatic budding zones, respectively. *Wnt5a*-positive staining is dark blue.

were maintained at 37 °C in a 95% air/5% CO_2 and 100% humidity incubator. MEFs were incubated for 1 h with 10 μM Calcium Green-1 AM (Molecular Probes, OR), washed with culture medium to remove unincorporated dye, and then maintained in 2 ml culture media for confocal fluorescent microscopy as described previously (Verbny et al., 2002). A 500× stock solution of rmWNT5A and anti-WNT5A-IgG were prepared in Hank's balanced Salt Solution (HBSS) and diluted into MEF culture media.

Real-time reverse-transcription PCR

Real-time reverse transcription polymerase chain reaction was performed as previously described (Lin et al., 2002). Primer sequences, annealing temperatures, and product sizes are provided in Supplemental Table 1.

Statistical analyses

Statistical analyses were performed using Statistica Software (StatSoft, Inc., Tulsa, OK). Levene's test was used to determine homogeneity of variances between or among groups with equal n values and the Brown–Forsythe test was used for groups with unequal n values. Student's t-test was used to identify differences between groups and one-way Analysis of Variance (ANOVA) to detect differences among groups. Fisher's Least Significant Test was used for multiple comparisons. A difference of $p<0.05$ was considered significant. Variances in mean bud number were not equal for all treatment groups (Levene's test $p<0.05$), so differences in bud number between groups were assessed using the nonparametric Mann–Whitney U test.

Results

Wnt5a is expressed in UGS mesenchyme during prostatic bud formation

Wnt5a is the most abundant *Wnt* transcript in the male mouse UGS during prostatic budding (Zhang et al., 2006) but its spatial distribution in the UGS has not been previously reported. We used ISH to investigate *Wnt5a* mRNA expression at 24 h intervals prior to and during prostatic budding (E15.5–17.5). Prior to bud initiation (E15.5), *Wnt5a* was detected in a diffuse band of UGM circumscribing each of the UGE zones from which prostatic buds emerge (Fig. 1). For each embryonic day examined, *Wnt5a* was most abundant in UGS zones where buds were forming and least abundant in non-budding regions of the UGS. *Wnt5a* was most abundant in the anterior budding zone immediately after anterior bud formation (E16.5), was moderately expressed in the dorsolateral prostatic budding zone during dorsolateral bud initiation, and was weakly expressed where buds had not yet emerged in the ventral budding zone at E16.5. *Wnt5a* staining on E17.5 appeared to be expressed at a much lower level in the ventral UGS region during ventral budding compared to that observed during budding from anterior and dorsolateral UGS regions. *Wnt5a* was also observed in UGM juxtaposed to elongating anterior and dorsal prostatic buds at E17.5, where expression was most robust at the base of buds and dissipated towards bud tips.

Wnt5a-null mice exhibit multiple urogenital abnormalities

The presence of *Wnt5a* transcripts in areas where anterior and dorsolateral prostatic buds were forming suggested it may be required for budding. To test this hypothesis, prostatic budding was assessed in wild-type (WT) and *Wnt5a* null mice at E18.5. Multiple urogenital abnormalities were associated with the *Wnt5a* null phenotype, including UGS agenesis in some fetuses. The incidence of specific defects is reported in Table 1. The UGS and bladder were absent and the hindgut ended blindly in approximately 30% of *Wnt5a* null male fetuses (results not shown). In the 70% of *Wnt5a* null male fetuses where the UGS was present, it was morphologically deformed, devoid of a pelvic urethra, and attached by a fistulous connection to the hindgut (Fig. 1, arrowheads).

Table 1
Incidence of urogenital defects in E18.5 *Wnt5a* null male fetuses

Type of defect[a]	*Wnt5a* null fetuses # affected/# observed
Undescended testes	14/14
Bladder agenesis	4/14
UGS agenesis	4/14
Pelvic urethra agenesis	9/14
Hindgut-UGS fistula[b]	10/10

[a] None of these defects were observed in wild type littermates ($n>14$).
[b] Results reported only for *Wnt5a* null fetuses in which the UGS had formed.

Three techniques were utilized to assess morphology in the most fully-developed UGSs from *Wnt5a* null males. First, intact UGSs of representative WT and E18.5 *Wnt5a* null male fetuses were photographed (Figs. 2A and C); second, a mid-sagittal UGS section from each genotype was examined histologically (Figs. 2B and D); and third, after the UGS was treated with trypsin and UGM was removed with fine forceps, the underlying UGE surface was examined by SEM and color coded to reveal anterior (red), dorsolateral (green) and ventral (yellow) prostatic buds (Fig. 3). The bladder neck and the prostatic urethra containing the anterior and ventral prostatic budding zones were truncated and widened in many *Wnt5a* null UGSs (Fig. 3). *Wnt5a* null UGSs exhibited prostatic bud patterning defects associated with this UGS deformity. Anterior buds were absent from all male *Wnt5a* null UGSs, ventral buds were rarely observed and dorsolateral bud number varied substantially between fetuses, but was always less than WT (Fig. 3).

Abnormal testicular development in Wnt5a *null* fetuses could impair prostatic budding by reducing circulating fetal testosterone. All fourteen *Wnt5a* null male fetuses examined exhibited defects in testicular descent. We therefore compared testicular testosterone content in WT and *Wnt5a* null fetuses to investigate testicular function in *Wnt5a* null fetuses. Loss of *Wnt5a* was associated with a significant reduction in fetal testicular testosterone (219±29 pg testosterone/testis in *Wnt5a* null fetuses vs. 732±116 pg testosterone/testis in WT fetuses, $p<0.05$).

WNT5A is not required for bud formation and exogenous WNT5A inhibits ventral budding

The *Wnt5a* null phenotype revealed a role for *Wnt5a* in the early phase of UGS morphogenesis and in UGS-hindgut separation. However, it was not possible to determine whether WNT5A was also required for prostatic budding or if prostatic budding defects in *Wnt5a* null fetuses occurred secondary to pre-existing UGS deformities and decreased testicular testosterone.

To determine if WNT5A signaling is directly required for prostatic bud formation, we assessed prostatic budding in a well-established, *in vitro* serum-free UGS organ culture model, where bladder neck and prostatic urethra morphology were normal at the start of the culture period and androgen concentration in the culture medium was sustained in the physiological range. Prostatic buds did not form in the absence of androgens (results not shown) and all subsequent

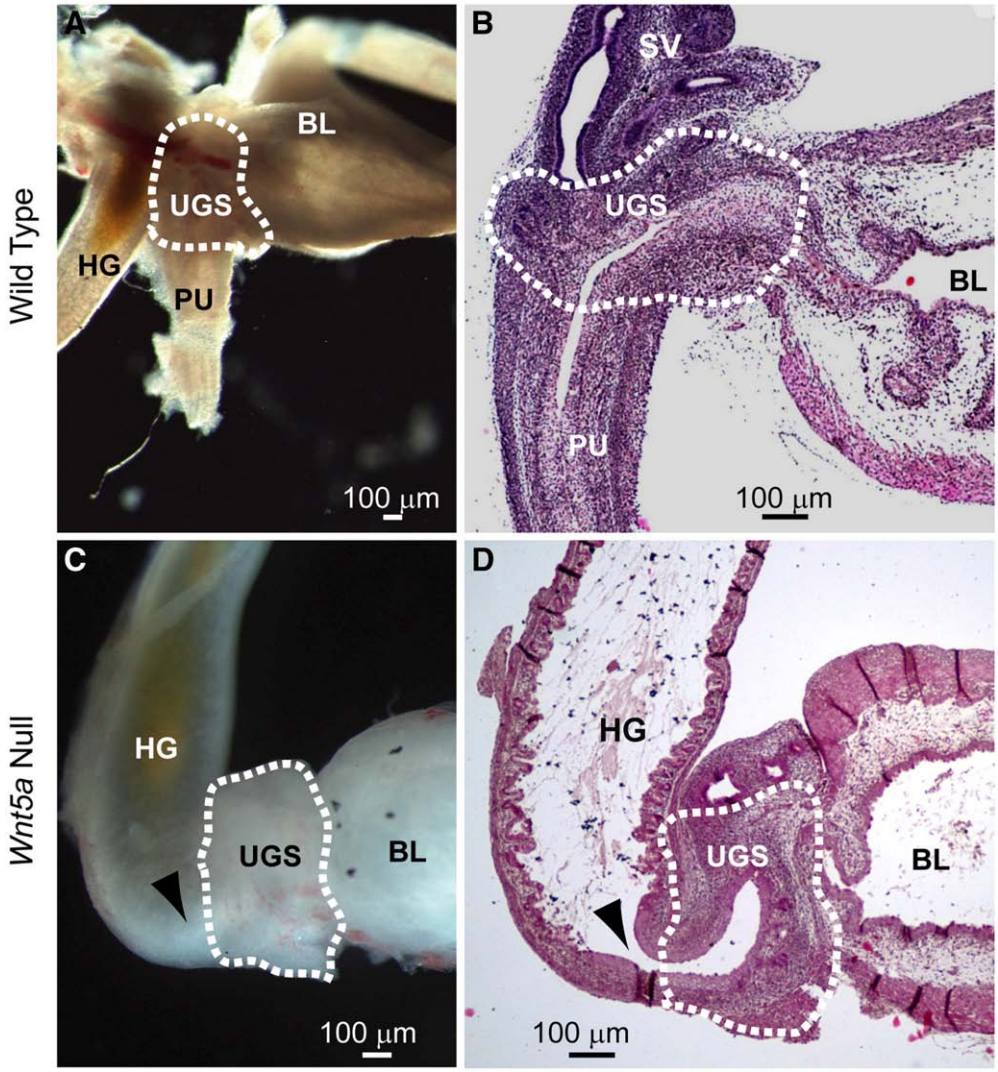

Fig. 2. E18.5 *Wnt5a* null male fetuses exhibit aberrant hindgut and urogenital morphology. Images of whole UGSs and hematoxylin and eosin stained sagittal UGS sections are shown for representative wild-type and *Wnt5a* null male mouse fetuses. Results are representative of ten fetuses from each genotype. Distal UGS boundaries are indicated by dashed white lines. The E18.5 *Wnt5a* null UGSs shown in panels C and D feature a fistulous hindgut (HG)-UGS connection (arrowhead) and agenic pelvic urethra (PU), compared to the normal anatomy of wild-type UGSs in panels A and B. The other structure shown is bladder (BL).

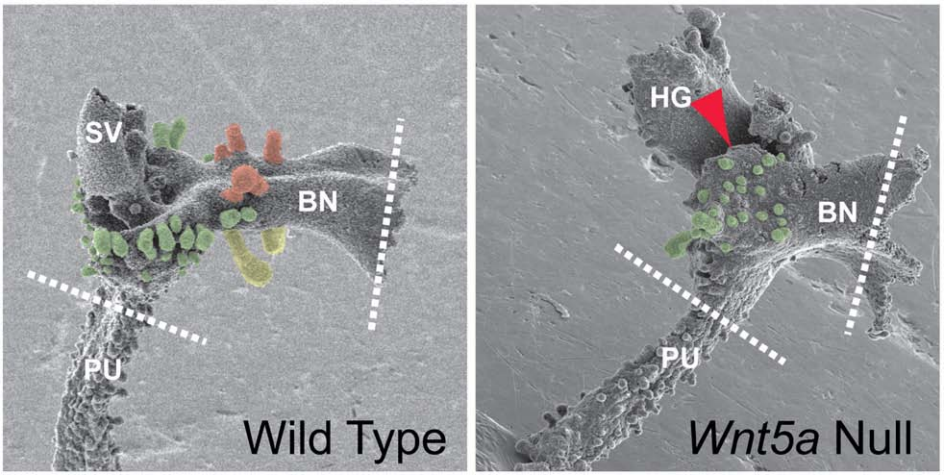

Fig. 3. E18.5 *Wnt5a* null male fetuses exhibit an aberrant prostatic bud pattern. UGS mesenchyme was removed from wild type and *Wnt5a* null UGSs and the underlying UGS epithelium (UGE) was visualized by scanning electron microscopy. Results are representative of three UGSs per genotype. The *Wnt5a* null UGE shown above exhibits a shortened and distended bladder neck (BN), is devoid of anterior (red) and ventral (yellow) prostatic buds, and exhibits fewer dorsolateral buds (green). Also evident is a fistulous connection (arrowhead) between UGS and hindgut (HG). HG is distinguished from seminal vesicle (SV) by its numerous epithelial protrusions. The other structure shown is the pelvic urethra (PU).

experiments were conducted with culture media containing 10 nM 5α-dihydrotestosterone (DHT, an AR agonist). WNT5A signaling in WT UGSs was then repressed by adding a WNT5A inhibitory antibody (anti-WNT5A-IgG) to the culture medium or was activated by adding recombinant mouse WNT5A (rmWNT5A) protein. These reagents were used previously to repress or activate WNT5A signaling in other systems (Castelo-Branco et al., 2006; Cheng et al., 2008; Dejmek et al., 2006; Murdoch et al., 2003; Roarty and Serra, 2007; Schulte et al., 2005). Their activities were confirmed in this study by measuring intracellular calcium mobilization (Supplemental Fig. 1) as a WNT5A-responsive endpoint (Ma and Wang, 2006; Schleiffarth et al., 2007).

We next incubated WT UGSs in organ culture media containing 10 nM DHT and vehicle or anti-WNT5A-IgG (4 and 8 μg/ml) to determine if WNT5A signaling was necessary for prostatic bud formation. Prostatic budding was assessed by removing UGM, imaging underlying UGE from multiple angles by SEM, and enumerating the total number of prostatic buds per UGS. Exposure to anti-WNT5A-IgG did not change the number of prostatic buds formed in culture (results not shown). This finding supports the hypothesis that WNT5A signaling is not required for prostatic bud formation.

Functional redundancy has been observed for some mediators of prostatic budding. For example, prostatic budding requires hedgehog signaling but occurs normally in *Shh* null mice because indian hedgehog is upregulated to compensate for loss of *Shh* (Doles et al., 2006). An analogous mechanism may also trigger the upregulation of a compensatory signal during *in vitro* incubation of UGSs with media containing anti-WNT5A-IgG, and this may explain why prostatic bud number was unchanged by treatment with anti-WNT5A-IgG. Therefore, as an alternative approach to interrogate the role of WNT5A in prostatic budding, we next investigated whether excess WNT5A signaling impaired prostatic bud formation. UGSs were cultured for 3 d with media containing 10 nM DHT and graded concentrations of exogenous rmWNT5A (0–2 μg/ml). Mean prostatic bud number was significantly reduced by rmWNT5A (1 and 2 μg/ml), to approximately 75% of the control value (Fig. 4). Inhibition of budding by rmWNT5A appeared to be AR independent since it did not significantly change *Ar* mRNA abundance or abundance of the androgen-responsive gene steroid 5 alpha-reductase 2 (results not shown).

Excess WNT5A signaling blocked the formation of some, but not all prostatic buds and we next investigated the hypothesis that WNT5A selectively blocked development of certain prostate buds and not others. UGSs were cultured for 3 d in the presence of vehicle (control) or an effective prostatic bud inhibitory concentration of rmWNT5A. UGSs were then grafted under the kidney capsules of adult male immunodeficient mice and allowed to grow for 28 d. Prostate lobar-development was assessed by histological examination and gene expression profiling. Relative mRNA abundance of prostate lobe-selective gene products was assessed by real-time RT-PCR. It was established previously that probasin (*Pbsn*) is selectively expressed in dorsal prostate, beta-microseminoprotein (*Msmb*) is selectively expressed in lateral prostate, renin 1 (*Ren1*) is selectively expressed in anterior prostate, and spermine binding protein (*Sbp*) is selectively expressed in ventral prostate (Cook et al., 2007; Fabian et al., 1993; Fujimoto et al., 2006; Kwong et al., 1999; Mills et al., 1987; Shi et al., 2007; Thielen et al., 2007; Xuan et al., 1999). Arborization of prostate ducts and cytodifferentiation of secretory luminal cells occurred

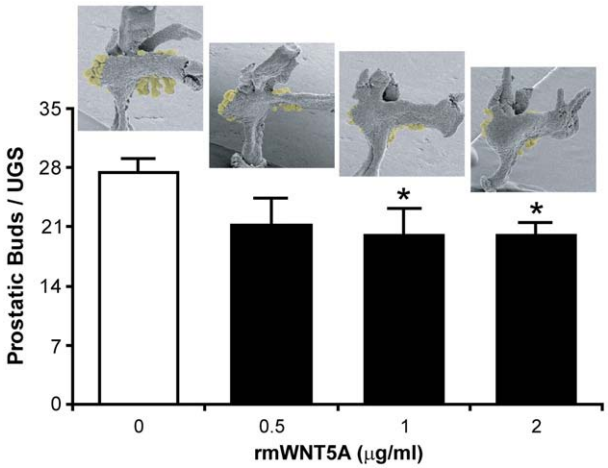

Fig. 4. Recombinant mouse WNT5A (rmWNT5A) restricts prostatic budding in mouse UGS organ culture. E14.5 UGSs were cultured for 3 d in serum-free media containing either 10 nM DHT and 0.1% DMSO (vehicle control, open bar) or DHT and graded concentrations of rmWNT5A (solid bars). Prostatic bud number (all lobes) was determined after the 3 d culture period by collecting each UGS, removing UGM as described previously, and then imaging the underlying UGE by scanning electron microscopy (SEM). A representative micrograph of a cultured UGS, after the mesenchyme was removed to reveal the underlying prostatic buds, is shown for each group. Prostatic buds are pseudocolored yellow. Results are mean ± SEM of five UGSs per group. Differences between groups were determined by ANOVA followed by Fisher's least-significant difference test. "*" indicates significantly different from the vehicle control (0 μg/ml rmWNT5A), $p<0.05$.

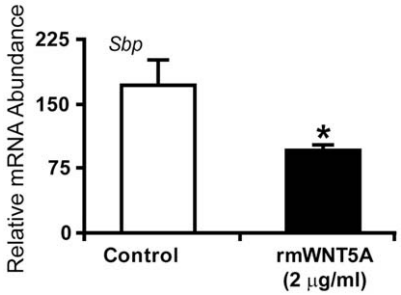

Fig. 5. Recombinant mouse WNT5A restricts ventral prostate development. E14.5 male UGSs were cultured for 3 d with 10 nM DHT, 0.1% DMSO and either no rmWNT5A (control, open bar) or 2 μg/ml rmWNT5A (solid bar) then grafted under the kidney capsule of adult male *nu/nu* mice and grown for 28 d. Real-time RT-PCR was used to measure abundance of a gene selectively expressed in ventral prostate, spermine binding protein (*Sbp*), as an index of ventral prostate development. The abundance of *Sbp* mRNA was normalized to peptidylprolyl isomerase A abundance, and results are presented as mean±SEM of five grafted UGSs per *in vitro* treatment. Differences between groups were determined by Student's *t* test. "*" indicates significantly different from vehicle control.

during this period in all grafted tissues. Grafted tissues from the rmWNT5A treatment group were devoid of ventral prostate ducts (results not shown) and exhibited significantly less *Sbp* (Fig. 5), despite the presence dorsolateral and anterior prostate ducts and normal levels of *Pbsn*, *Msmb*, and *Ren1* (results not shown).

Antagonism of WNT5A signaling reverses ventral prostate inhibition by TCDD

To independently confirm that WNT5A acts selectively to block development of ventral prostate, but not other lobes, we investigated the effect of anti-WNT5A-IgG in a chemical model of ventral prostatic budding inhibition. We demonstrated previously that ventral prostatic budding was selectively impaired by TCDD, an agonist of the AHR nuclear orphan receptor and transcription factor (Lin et al., 2003). Since TCDD inhibits budding in a ventral UGS-selective fashion, we hypothesized that inhibition of WNT5A signaling may rescue ventral prostatic budding from inhibition by TCDD. UGSs were incubated for 3 d in organ culture media containing DHT and vehicle (control), TCDD, or TCDD+ anti-WNT5A-IgG. TCDD alone significantly reduced total prostatic bud number and this effect was blocked by anti-WNT5A-IgG (Fig. 5A). To test whether this restoration of bud number by anti-WNT5A-IgG was due to the rescue of ventral bud formation, UGSs from the treatment groups described above were grafted under the kidney capsule of immunodeficient mice and evaluated 28 d later. Based on histological assessment and expression of transcripts that are selectively expressed in each of the mouse prostate lobes, TCDD did not impair development of anterior or dorsolateral prostate (results not shown). The antibody alone did not significantly change prostatic bud number or impair development of anterior, dorsolateral, or ventral prostate (results not shown). However, TCDD selectively impaired development of ventral prostate and this was restored by inhibition of WNT5A signaling with anti-WNT5A-IgG (Fig. 6). Thus, inhibition of WNT5A signaling reverses the inhibitory actions of TCDD on ventral prostatic budding.

Discussion

WNT5A is required for early events in urogenital development

This is the first report, to our knowledge, that WNT5A is required early in testes, bladder, pelvic urethra, and UGS formation. *Wnt5a* null male mouse fetuses exhibited less testicular testosterone and thirty percent did not form bladder or pelvic urethra. Of the 70% of *Wnt5a* null male fetuses that formed bladder and UGS, only half formed pelvic urethra. It is worthwhile to note that agenesis of bladder, pelvic urethra, and UGS was not gender-dependent and occurred at the same frequency in male and female *Wnt5a* null mice (unpublished observation).

Prostatic budding was impaired in *Wnt5a* null male mice. However, we were unable to replicate this aberrant budding phenotype by pharmacologically inhibiting WNT5A signaling in WT UGSs cultured in media containing anti-WNT5A-IgG. Our interpretation of these results is that *Wnt5a* may contribute to, but alone is not required for prostatic bud patterning. Instead, *Wnt5a* may be required for normal UGS morphogenesis prior to budding. We suggest that truncation and distention of anterior and ventral prostatic budding zones in *Wnt5a* null males and decreased testosterone production predisposed these mice to bud patterning defects that do not occur in morphologically normal, WT UGSs. It was shown long ago that ventral prostatic buds are the most sensitive to androgen. Ventral prostatic buds form in female UGSs (Raynaud, 1942) even though circulating androgens are lower than in males (vom Saal, 1989). Androgens induce prostatic budding in female rats, with ventral prostatic bud formation occurring at lower androgen doses compared to dorsolateral and anterior buds (Greene et al., 1939). Therefore, absence of ventral buds in *Wnt5a* null UGSs suggests that other factors, in addition to reduced testosterone levels in these fetuses, contribute to ventral bud agenesis in these mice.

Excess Wnt5a negatively regulates ventral prostate development

Mechanisms responsible for prostatic bud patterning are poorly understood. The significance of our work is that it is the first to report impairment of ventral prostatic bud specification by WNT5A, the

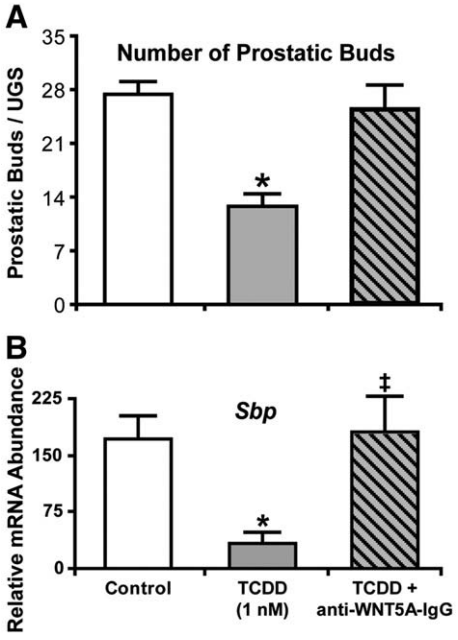

Fig. 6. A WNT5A inhibitory antibody (anti-WNT5A-IgG) counteracts the effects of a selective ventral prostate inhibitor, TCDD, during mouse UGS development *in vitro*. E14.5 UGSs were cultured for 3 d in serum-free media containing 10 nM DHT and 0.1% DMSO (vehicle control, open bar) or these same two constituents and either TCDD (1 nM, gray-shaded bar) or TCDD+ anti-WNT5A-IgG (gray-shaded, diagonally slashed bar). (A) Some cultured UGSs were imaged by scanning electron microscopy to assess total bud count. (B) Other cultured UGSs were grafted under the kidney capsule of *nu/nu* mice and grown for 28 d. Ventral prostate development was assessed by using real-time, RT-PCR to measure abundance of the ventral prostate-selective transcript, spermine binding protein (*Sbp*), in grafted tissues. *Sbp* abundance was normalized to peptidylprolyl isomerase A. Results are mean±SEM of five UGS per treatment group. Differences between groups were determined by ANOVA followed by Fisher's least significant difference test. The presence of "*" indicates significantly different from vehicle control and "‡" indicates significantly different from TCDD ($p<0.05$).

prototypical non-canonical WNT protein. Effects of WNT5A on prostatic budding are strikingly similar to those produced by TCDD, a previously identified chemical inhibitor of ventral prostatic budding and potent ligand of the AHR. We showed previously that AHR signaling was not required for prostatic bud formation (Lin et al., 2003) and showed in this study that WNT5A signaling also was not required for prostatic budding *in vitro*. However, activation of either AHR or WNT5A signaling inhibited budding. Addition of rmWNT5A or TCDD to UGS organ culture meida blocked ventral prostate development, as assessed by *Sbp* abundance and ventral prostate duct formation in grafted tissues. The blockade of prostate development by rmWNT5A and TCDD was ventral prostate-selective and did not appreciably affect dorsolateral or anterior prostate development. Inhibition of WNT5A signaling during UGS organ culture with TCDD completely prevented the loss of buds associated with TCDD exposure and permitted ventral prostate development. Collectively, these results support our hypothesis that WNT5A is a ventral UGS region-selective inhibitor of ventral prostate development in mice.

SOX9 was recently identified as a prostatic bud inhibitor (Thomsen et al., 2008). Conditional deletion of *Sox9* in cells that express the early prostate marker NKX3.1 prevented ventral prostatic buds from forming while having considerably lesser effects on prostatic budding in other UGS regions. Since mesenchymal–epithelial interactions are required for prostatic budding (Cunha and Chung, 1981) and *Wnt5a* is synthesized in UGS mesenchyme, SOX9 activity in UGS epithelium may be mechanistically linked and downstream of WNT5A signaling during prostatic bud formation.

Wnt5a overlaps Ar, Bmp4, and Hoxa13 during prostate specification

Formation of bladder and UGS are supported by hormonally-independent developmental pathways but prostatic bud patterning and initiation require androgen (Lasnitzki and Mizuno, 1980). ARs in UGM bind testosterone but in UGE do not (Takeda and Chang, 1991). Activation of ARs in the periprostatic portion of UGM is particularly important for prostate specification (Takeda et al., 1987). *Wnt5a* abundance was not directly regulated by androgens (results not shown) but did overlap the purported location of AR activity. We detected *Wnt5a* in periprostatic UGM prior to and during bud formation. In UGS organ culture, rmWNT5A inhibited prostatic budding without changing abundance of *Ar* mRNA or abundance of *Srd5a2*, a gene that is directly regulated by activated AR. Thus, inhibition of prostatic budding by exogenous WNT5A likely occurred downstream of AR signaling.

Wnt5a is not required for prostatic budding *in vivo*. However, *Wnt5a* mRNA is up-regulated in anterior, dorsolateral, and ventral UGS budding zones during bud formation in these regions. Coupled with the fact that exogenous rmWNT5A inhibits prostatic budding, the functional role of WNT5A during prostatic budding *in vivo* may be to act in concert with other factors to limit the total number of buds that form in each UGS zone, especially the ventral budding zone. A similar role has been ascribed to *Bmp4*, which is also expressed in UGM during budding and inhibits prostatic budding from cultured UGSs (Lamm et al., 2001; Vezina et al., 2008). In future studies, we will investigate interaction between *Wnt5a* and *Bmp4* during prostatic budding, since these factors appear to be involved in a signaling loop in other tissues: *Wnt5a* is required for *Bmp4* expression in developing mouse lung (Li et al., 2002) and *Bmp4* is required for *Wnt5a* expression in the genital tubercle (Oishi et al., 2003).

Hoxa13, which is required at least in part for normal prostatic bud patterning (Warot et al., 1997), appears to functionally overlap *Wnt5a* during uterine development (Mericskay et al., 2004) and has recently been shown to control *Wnt5a* expression in mouse dermal fibroblasts (Rinn et al., 2008). The pattern of *Wnt5a* expression overlaps with *Hoxa13* in the UGS (Warot et al., 1997), raising the possibility that *Hoxa13* may interact with *Wnt5a* during prostatic budding. Further characterization of the regulatory loop between these signaling molecules may provide clues for how patterning of ventral, as well as dorsolateral and anterior prostatic budding, is achieved.

Acknowledgments

This publication was supported by National Institutes of Health grants F31-HD049323 (SHA), F32-ES014284 (CMV), R37-ES01332 (REP), and T32-ES07015 (Molecular and Environmental Toxicology Center). The authors thank Dr. Terry Yamaguchi (NCI, Frederick, MD) for providing *Wnt5a* null breeders and *Wnt5a* probe for *in situ* hybridization, and thank Dr. Ralph Albrecht and the Biological and Bio-materials Preparation, Imaging, and Characterization Laboratory (UW-Madison) for assistance with scanning electron microscopy.

Appendix A. Supplementary data

Supplementary data associated with this article can be found, in the online version, at doi:10.1016/j.ydbio.2008.08.018.

References

Benedict, J.C., Lin, T.M., Loeffler, I.K., Peterson, R.E., Flaws, J.A., 2000. Physiological role of the aryl hydrocarbon receptor in mouse ovary development. Toxicol. Sci. 56, 382–388.

Castelo-Branco, G., Sousa, K.M., Bryja, V., Pinto, L., Wagner, J., Arenas, E., 2006. Ventral midbrain glia express region-specific transcription factors and regulate dopaminergic neurogenesis through Wnt-5a secretion. Mol. Cell. Neurosci. 31, 251–262.

Cheng, C.W., Yeh, J.C., Fan, T.P., Smith, S.K., Charnock-Jones, D.S., 2008. Wnt5a-mediated non-canonical Wnt signalling regulates human endothelial cell proliferation and migration. Biochem. Biophys. Res. Commun. 365, 285–290.

Cook, C., Vezina, C.M., Allgeier, S.H., Shaw, A., Yu, M., Peterson, R.E., Bushman, W., 2007. Noggin is required for normal lobe patterning and ductal budding in the mouse prostate. Dev. Biol. 312, 217–230.

Cunha, G.R., Chung, L.W., 1981. Stromal–epithelial interactions-I. Induction of prostatic phenotype in urothelium of testicular feminized (Tfm/y) mice. J. Steroid Biochem. 14, 1317–1324.

Cunha, G.R., Lung, B., 1978. The possible influence of temporal factors in androgenic responsiveness of urogenital tissue recombinants from wild-type and androgen-insensitive (*Tfm*) mice. J. Exp. Zool. 205, 181–193.

Cunha, G.R., Donjacour, A.A., Cooke, P.S., Mee, S., Bigsby, R.M., Higgins, S.J., Sugimura, Y., 1987. The endocrinology and developmental biology of the prostate. Endocr. Rev. 8, 338–362.

Dejmek, J., Safholm, A., Kamp Nielsen, C., Andersson, T., Leandersson, K., 2006. Wnt-5a/Ca2+-induced NFAT activity is counteracted by Wnt-5a/Yes-Cdc42-casein kinase 1alpha signaling in human mammary epithelial cells. Mol. Cell. Biol. 26, 6024–6036.

Doles, J., Cook, C., Shi, X., Valosky, J., Lipinski, R., Bushman, W., 2006. Functional compensation in Hedgehog signaling during mouse prostate development. Dev. Biol. 295, 13–25.

Donjacour, A.A., Thomson, A.A., Cunha, G.R., 2003. FGF-10 plays an essential role in the growth of the fetal prostate. Dev. Biol. 261, 39–54.

Fabian, J.R., Kane, C.M., Abel, K.J., Gross, K.W., 1993. Expression of the mouse Ren-1 gene in the coagulating gland: localization and regulation. Biol. Reprod. 48, 1383–1394.

Fujimoto, N., Akimoto, Y., Suzuki, T., Kitamura, S., Ohta, S., 2006. Identification of prostatic-secreted proteins in mice by mass spectrometric analysis and evaluation of lobe-specific and androgen-dependent mRNA expression. J. Endocrinol. 190, 793–803.

Gat, U., DasGupta, R., Degenstein, L., Fuchs, E., 1998. De Novo hair follicle morphogenesis and hair tumors in mice expressing a truncated beta-catenin in skin. Cell 95, 605–614.

Goldstein, J.L., Wilson, J.D., 1975. Genetic and hormonal control of male sexual differentiation. J. Cell. Physiol. 85, 365–377.

Greene, R.R., Burrill, M.W., Ivy, A.C., 1939. Experimental intersexuality. The effect of antenatal androgens on sexual development in female rats. Amer. J. Anat. 65, 415–469.

Grishina, I.B., Kim, S.Y., Ferrara, C., Makarenkova, H.P., Walden, P.D., 2005. BMP7 inhibits branching morphogenesis in the prostate gland and interferes with Notch signaling. Dev. Biol. 288, 334–347.

Hogan, B.L., 1999. Morphogenesis. Cell 96, 225–233.

Joesting, M.S., Cheever, T.R., Volzing, K.G., Yamaguchi, T.P., Wolf, V., Naf, D., Rubin, J.S., Marker, P.C., 2008. Secreted frizzled related protein 1 is a paracrine modulator of epithelial branching morphogenesis, proliferation, and secretory gene expression in the prostate. Dev. Biol. 317, 161–173.

Kwong, J., Chan, F.L., Jiang, S., Guo, Y., Imasato, Y., Sakai, H., Koropatnick, J., Chin, J.L., Xuan, J.W., 1999. Differential expression of PSP94 in rat prostate lobes as demonstrated by an antibody against recombinant GST-PSP94. J. Cell. Biochem. 74, 406–417.

Lamm, M.L., Podlasek, C.A., Barnett, D.H., Lee, J., Clemens, J.Q., Hebner, C.M., Bushman, W., 2001. Mesenchymal factor bone morphogenetic protein 4 restricts ductal budding and branching morphogenesis in the developing prostate. Dev. Biol. 232, 301–314.

Lamm, M.L., Catbagan, W.S., Laciak, R.J., Barnett, D.H., Hebner, C.M., Gaffield, W., Walterhouse, D., Iannaccone, P., Bushman, W., 2002. Sonic hedgehog activates mesenchymal Gli1 expression during prostate ductal bud formation. Dev. Biol. 249, 349–366.

Lasnitzki, I., Mizuno, T., 1980. Prostatic induction: interaction of epithelium and mesenchyme from normal wild-type mice and androgen-insensitive mice with testicular feminization. J. Endocrinol. 85, 423–428.

Li, C., Xiao, J., Hormi, K., Borok, Z., Minoo, P., 2002. Wnt5a participates in distal lung morphogenesis. Dev. Biol. 248, 68–81.

Lin, T.M., Ko, K., Moore, R.W., Buchanan, D.L., Cooke, P.S., Peterson, R.E., 2001. Role of the aryl hydrocarbon receptor in the development of control and 2,3,7,8-tetrachlorodibenzo-p-dioxin-exposed male mice. J. Toxicol. Environ. Health, A 64, 327–342.

Lin, T.M., Ko, K., Moore, R.W., Simanainen, U., Oberley, T.D., Peterson, R.E., 2002. Effects of aryl hydrocarbon receptor null mutation and in utero and lactational 2,3,7,8-tetrachlorodibenzo-p-dioxin exposure on prostate and seminal vesicle development in C57BL/6 mice. Toxicol. Sci. 68, 479–487.

Lin, T.M., Rasmussen, N.T., Moore, R.W., Albrecht, R.M., Peterson, R.E., 2003. Region-specific inhibition of prostatic epithelial bud formation in the urogenital sinus of C57BL/6 mice exposed in utero to 2,3,7,8-tetrachlorodibenzo-p-dioxin. Toxicol. Sci. 76, 171–181.

Liu, F., Thirumangalathu, S., Gallant, N.M., Yang, S.H., Stoick-Cooper, C.L., Reddy, S.T., Andl, T., Taketo, M.M., Dlugosz, A.A., Moon, R.T., Barlow, L.A., Millar, S.E., 2007. Wnt-beta-catenin signaling initiates taste papilla development. Nat. Genet. 39, 106–112.

Liu, F., Chu, E.Y., Watt, B., Zhang, Y., Gallant, N.M., Andl, T., Yang, S.H., Lu, M.M., Piccolo, S., Schmidt-Ullrich, R., Taketo, M.M., Morrisey, E.E., Atit, R., Dlugosz, A.A., Millar, S.E., 2008. Wnt/beta-catenin signaling directs multiple stages of tooth morphogenesis. Dev. Biol. 313, 210–224.

Lu, Y., Zhang, J., Dai, J., Dehne, L.A., Mizokami, A., Yao, Z., Keller, E.T., 2004. Osteoblasts induce prostate cancer proliferation and PSA expression through interleukin-6-mediated activation of the androgen receptor. Clin. Exp. Metastasis 21, 399–408.

Ma, L., Wang, H.Y., 2006. Suppression of cyclic GMP-dependent protein kinase is essential to the Wnt/cGMP/Ca2+pathway. J. Biol. Chem. 281, 30990–31001.

Mericskay, M., Kitajewski, J., Sassoon, D., 2004. Wnt5a is required for proper epithelial-mesenchymal interactions in the uterus. Development 131, 2061–2072.

Mills, J.S., Needham, M., Thompson, T.C., Parker, M.G., 1987. Androgen-regulated expression of secretory protein synthesis in mouse ventral prostate. Mol. Cell. Endocrinol. 53, 111–118.

Murdoch, B., Chadwick, K., Martin, M., Shojaei, F., Shah, K.V., Gallacher, L., Moon, R.T., Bhatia, M., 2003. Wnt-5A augments repopulating capacity and primitive hematopoietic development of human blood stem cells in vivo. Proc. Natl. Acad. Sci. U. S. A. 100, 3422–3427.

Noramly, S., Freeman, A., Morgan, B.A., 1999. beta-catenin signaling can initiate feather bud development. Development 126, 3509–3521.

Oishi, I., Suzuki, H., Onishi, N., Takada, R., Kani, S., Ohkawara, B., Koshida, I., Suzuki, K., Yamada, G., Schwabe, G.C., Mundlos, S., Shibuya, H., Takada, S., Minami, Y., 2003. The receptor tyrosine kinase Ror2 is involved in non-canonical Wnt5a/JNK signalling pathway. Genes Cells 8, 645–654.

Podlasek, C.A., Barnett, D.H., Clemens, J.Q., Bak, P.M., Bushman, W., 1999a. Prostate development requires Sonic hedgehog expressed by the urogenital sinus epithelium. Dev. Biol. 209, 28–39.

Podlasek, C.A., Clemens, J.Q., Bushman, W., 1999b. Hoxa-13 gene mutation results in abnormal seminal vesicle and prostate development. J. Urol. 161, 1655–1661.

Raynaud, A., 1942. Recherches embryologiques et histologiques sur la différenciation sexuelle normale de la souris. Bull. Biol. Fr. Belg. 29, 1–114 Suppl.

Rinn, J.L., Wang, J.K., Allen, N., Brugmann, S.A., Mikels, A.J., Liu, H., Ridky, T.W., Stadler, H.S., Nusse, R., Helms, J.A., Chang, H.Y., 2008. A dermal HOX transcriptional program regulates site-specific epidermal fate. Genes Dev. 22, 303–307.

Roarty, K., Serra, R., 2007. Wnt5a is required for proper mammary gland development and TGF-beta-mediated inhibition of ductal growth. Development 134, 3929–3939.

Schleiffarth, J.R., Person, A.D., Martinsen, B.J., Sukovich, D.J., Neumann, A., Baker, C.V., Lohr, J.L., Cornfield, D.N., Ekker, S.C., Petryk, A., 2007. Wnt5a is required for cardiac outflow tract septation in mice. Pediatr. Res. 61, 386–391.

Schulte, G., Bryja, V., Rawal, N., Castelo-Branco, G., Sousa, K.M., Arenas, E., 2005. Purified Wnt-5a increases differentiation of midbrain dopaminergic cells and dishevelled phosphorylation. J. Neurochem. 92, 1550–1553.

Shi, X., Gipp, J., Bushman, W., 2007. Anchorage-independent culture maintains prostate stem cells. Dev. Biol. 312, 396–406.

Takeda, H., Chang, C., 1991. Immunohistochemical and in-situ hybridization analysis of androgen receptor expression during the development of the mouse prostate gland. J. Endocrinol. 129, 83–89.

Takeda, H., Lasnitzki, I., Mizuno, T., 1987. Change of mosaic pattern by androgens during prostatic bud formation in XTfm/X+heterozygous female mice. J. Endocrinol. 114, 131–137.

Teuliere, J., Faraldo, M.M., Deugnier, M.A., Shtutman, M., Ben-Ze'ev, A., Thiery, J.P., Glukhova, M.A., 2005. Targeted activation of beta-catenin signaling in basal mammary epithelial cells affects mammary development and leads to hyperplasia. Development 132, 267–277.

Thielen, J.L., Volzing, K.G., Collier, L.S., Green, L.E., Largaespada, D.A., Marker, P.C., 2007. Markers of prostate region-specific epithelial identity define anatomical locations in the mouse prostate that are molecularly similar to human prostate cancers. Differentiation 75, 49–61.

Thomsen, M.K., Butler, C.M., Shen, M.M., Swain, A., 2008. Sox9 is required for prostate development. Dev. Biol. 316, 302–311.

Timms, B.G., Howdeshell, K.L., Barton, L., Bradley, S., Richter, C.A., vom Saal, F.S., 2005. Estrogenic chemicals in plastic and oral contraceptives disrupt development of the fetal mouse prostate and urethra. Proc. Natl. Acad. Sci. U. S. A. 102, 7014–7019.

Verbny, Y., Zhang, C.L., Chiu, S.Y., 2002. Coupling of calcium homeostasis to axonal sodium in axons of mouse optic nerve. J. Neurophysiol. 88, 802–816.

Vezina, C.M., Allgeier, S.H., Fritz, W.A., Moore, R.W., Strerath, M., Bushman, W., Peterson, R.E., 2008. Retinoic acid induces prostatic bud formation. Dev. Dyn.

Vezina, C.M., Allgeier, S.H., Moore, R.W., Lin, T.M., Bemis, J.C., Hardin, H.A., Gasiewicz, T.A., Peterson, R.E., in press. Dioxin causes ventral prostate agenesis by disrupting dorsoventral patterning in developing mouse prostate. Toxicol. Sci. doi:10.1093/toxsci/kfn183.

vom Saal, F.S., 1989. Sexual differentiation in litter-bearing mammals: influence of sex of adjacent fetuses in utero. J. Anim. Sci. 67, 1824–1840.

Warot, X., Fromental-Ramain, C., Fraulob, V., Chambon, P., Dolle, P., 1997. Gene dosage-dependent effects of the Hoxa-13 and Hoxd-13 mutations on morphogenesis of the terminal parts of the digestive and urogenital tracts. Development 124, 4781–4791.

Widelitz, R.B., Jiang, T.X., Lu, J., Chuong, C.M., 2000. beta-catenin in epithelial morphogenesis: conversion of part of avian foot scales into feather buds with a mutated beta-catenin. Dev. Biol. 219, 98–114.

Xuan, J.W., Kwong, J., Chan, F.L., Ricci, M., Imasato, Y., Sakai, H., Fong, G.H., Panchal, C., Chin, J.L., 1999. cDNA, genomic cloning, and gene expression analysis of mouse PSP94 (prostate secretory protein of 94 amino acids). DNA Cell Biol. 18, 11–26.

Yamaguchi, T.P., Bradley, A., McMahon, A.P., Jones, S., 1999. A Wnt5a pathway underlies outgrowth of multiple structures in the vertebrate embryo. Development 126, 1211–1223.

Zhang, T.J., Hoffman, B.G., Ruiz de Algara, T., Helgason, C.D., 2006. SAGE reveals expression of Wnt signalling pathway members during mouse prostate development. Gene Expr. Patterns 6, 310–324.